ARTICLE

Corrosion Study on Tantalum in Anhydrous Ethanol

Hai-ping Yang[a*], Mo-tang Tang[b], Bi-hui Li[a]

a. College of Chemistry and Materials Science, Hubei Engineering University, Xiaogan 432000, China
b. School of Metallurgical Science and Engineering, Central South University, Changsha 410083, China

(Dated: Received on April 28, 2014; Accepted on July 2, 2014)

The corrosion behavior of tantalum in tetraethyl ammonium chloride (TEA) ethanol solutions was investigated using potentiodynamic polarization, cyclic voltammetry, and impedance techniques along with scanning electron microscopy (SEM). At the early stage of scanning, the current density in the cyclic voltammetry curves very slowly increased because of the presence of a thin oxide film on the electrode surface. Pitting corrosion then occurred as a result of the passivity breakdown caused by the aggressive attack of the Cl^- anions. SEM images showed the growth process of the pits on the electrode surface. The pitting potential decreased with the increase in TEA concentration but increased with the increase in water concentration. The apparent activation energy of the electrochemical reaction was 36 kJ/mol. The impedance spectra exhibited two time constants for all the potentials. Both the passive layer resistance and the charge transfer resistance decreased with the increase in the potential.

Key words: Anhydrous ethanol, Electrochemical, Tantalum, Pitting corrosion

I. INTRODUCTION

Tantalum pentoxide (Ta_2O_5) has received considerable attention over the past decades because of its high dielectric constant (about 25), high refractive index, chemical and thermal stability, compatibility with ultra-large scale integrated circuits, and promising application to MOM or MOS capacitors, waveguides, silicon solar cells, and electrochromic devices and displays [1−4]. Ta_2O_5 films have been deposited through chemical vapor deposition using several precursor materials, such as $Ta(OC_2H_5)_5$, $Ta(OCH_3)_5$, $TaCl_5$, and $Ta[N(CH_3)_2]_5$. Among these precursors, tantalum ethoxide is the most preferred because of its 100% volatility and superior thermal stability [5].

The most common, technically simplest, and most economic preparation of tantalum alkoxides is based on tantalum chloride and alcohol [6]. However, this method has the disadvantage of liberating HCl gas, resulting in the severe corrosion of the reaction apparatus. The reaction is performed using large amounts of organic solvents, which are costly to dispose. Moreover, the necessary reagents are scarce, and the reactions involve various side processes that contaminate the products and decrease their yields [7].

For these reasons, the direct electrochemical synthesis of metal alkoxides seems to be a very promising method. This synthesis is conducted through the anode dissolution of metals in absolute alcohols in the presence of a conductive admixture. The electrochemical method has great potential for the direct conversion of less electropositive metals to their alkoxides because it is simple, highly productivity, continuous, and non-pollutive (with hydrogen as the major by-product) [8].

In 1972, the electrochemical synthesis of tantalum ethoxide was patented; it was done through the anodic dissolution of tantalum (Ta) in ethanol in the presence of tetraethyl ammonium chloride (TEA) as the electroconductive additive [9]. Since then, tantalum ethoxide was prepared by Shreider *et al.* [10], Turova *et al.* [11], and Yang *et al.* [12−15] using the electrochemical method. The electrochemical technique appears to have been successfully used in Russia for the commercial production of the alkoxides of Y, Ti, Zr, Nb, Ta, Mo, W, Cu, Ge, Sn, and other metals [8].

Despite the extensive studies on the electrochemical synthesis of tantalum ethoxide, the formation mechanism of the alkoxide is still unclear and only a few studies have been reported on the corrosion behavior of this process [16−18].

In the present work, the corrosion behavior of Ta in anhydrous ethanol containing supporting electrolytes was investigated using potentiodynamic polarization, cyclic voltammetry, and impedance techniques, which are useful in understanding the reaction mechanism and choosing the synthesis parameters.

*Author to whom correspondence should be addressed. E-mail: yhp1008@163.com, Tel.: +86-712-2345464

II. EXPERIMENTS

A. Materials and pretreatment of electrode

A tantalum rod (ø2.25 mm×180 mm) was supplied by Zhuzhou Cemented Carbide Group Corp. Ltd., with a chemical composition (wt%): O 0.02, C 0.005, N 0.003, Fe 0.005, Ni 0.005, Cr 0.005, Nb 0.002, W 0.002, Mo 0.001, Si 0.002, Mn 0.001, and Ta balance. The apparent exposed area was 0.25 cm^2. The electrode was successively polished with a series of emery papers, from a coarse one 400 to fine grade 1200, rinsed with acetone, ethanol, and finally dipped in the electrolytic cell.

B. Electrochemical measurements

The experiments were performed in a 300 mL Pyrex glass cell using Pt foil and a saturated calomel electrode (SCE) as the auxiliary and reference electrodes, respectively. To avoid contamination, the SCE was connected to a bridge filled with the solution during the test, the tip of which was pressed against the surface of the working electrode to minimize IR drop. All potentials given in this work refer to this electrode. All chemicals used were of analytically pure grade. The electrolyte solutions were prepared from anhydrous ethanol and TEA. Prior to the experiments, the solutions were deaerated using N_2, and the electrode was kept at −1 V for 300 s to electro-reduce any possible oxidized surface species.

Electrochemical measurements were performed using a potentiostat/galvanostat (CHI 660C Electrochemical Workstation, provided by Shanghai CH Instrument Company, China) connected to a personal computer. The potentiodynamic polarization curves were recorded by automatically changing the electrode potential from −1.0 V to 3.0 V at the desired scan rate. Cyclic voltammetric measurements were conducted by linearly sweeping the potential from the starting potential to the positive direction at the given scan rate up to the required potential value. Then, the same scan rate is reversed to the starting potential to form one complete cycle. The current density is the current divided by the exposed geometric surface area which is calculated by the diameter of the tantalum rod. Electrochemical impedance spectra (EIS) measurements were taken using AC signals of 5 mV amplitude at a certain potential in the frequency range of 100 kHz to 0.01 Hz. The EIS results were analyzed using Zview software. Each experiment was performed with freshly prepared solutions and newly polished sets of electrodes. All measurements were carried out at room temperature (25±1 °C) and repeated twice.

C. SEM characterization of electrode surface

The electrode surface was examined by the scanning electron microscope (SEM model JSM-6360 LV) after anodization at 2.5 V for various time in 0.1 mol/L TEA ethanol solution.

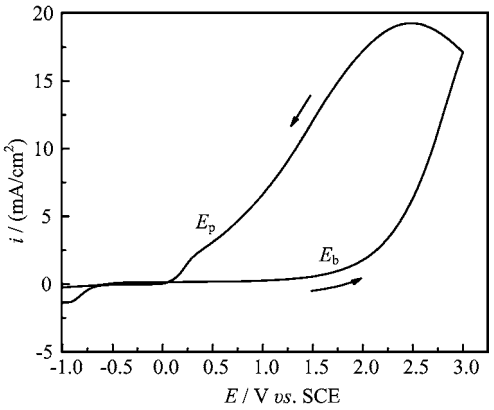

FIG. 1 A typical cyclic voltammogram of Ta in anhydrous ethanol containing 0.06 mol/L TEA with a scan rate of 50 mV/s.

III. RESULTS AND DISCUSSION

A. Typical potentiodynamic polarization curve

Figure 1 displays the potentiodynamic polarization curve of Ta in anhydrous ethanol containing 0.06 mol/L TEA. On the positive scan, the cathodic current density decreased, gradually forming a small cathodic current plateau just before reaching a zero value at the corrosion potential (E_{corr}). This plateau probably corresponds to the hydrogen evolution reaction on the Ta surface. The current density very slowly increased with anodic potential. This phenomenon could be attributed to the spontaneous passivation of Ta because of the presence of the oxide film on the electrode surface. In fact, Ta itself is an active metal from an electrochemical point of view because its domain of thermodynamic stability is known to lie below that of water reduction at temperatures from 25 °C to 300 °C [19]. Ta dissolution may occur through the chemical dissolution of the protective passive oxide film. With the increase in anodic potential, the passive current density gradually increased, indicating that the chemical dissolution accelerated.

However, when the anodic potential exceeded a certain critical value E_b, the current density suddenly increased without any sign of oxygen evolution, suggesting the breakdown of the passive film and the initiation and propagation of the pitting corrosion. The current density continued even after the potential sweep reversal, which is an autocatalytic characteristic of pitting [20]. Afterwards, the current density began to linearly decay. A hysteresis loop, which is a characteristic of the pitting corrosion phenomenon, was formed [21]. This hysteresis loop enabled the repassivation potential E_p to be determined, where E_p corresponds to the potential values below which no pitting occurs and above which

DOI:10.1063/1674-0068/27/04/491-496

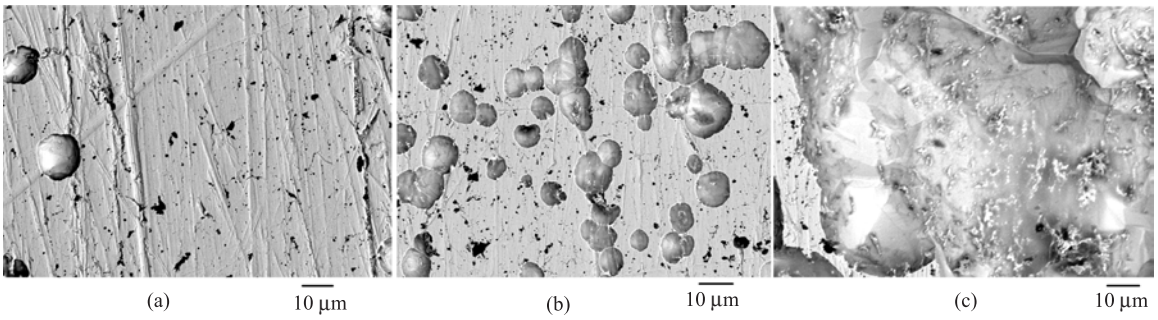

FIG. 2 SEM microphotographs of Ta surface after anodization at 2.5 V for various time in 0.1 mol/L TEA ethanol solution. (a) 2 min, (b) 5 min, (c) 60 min.

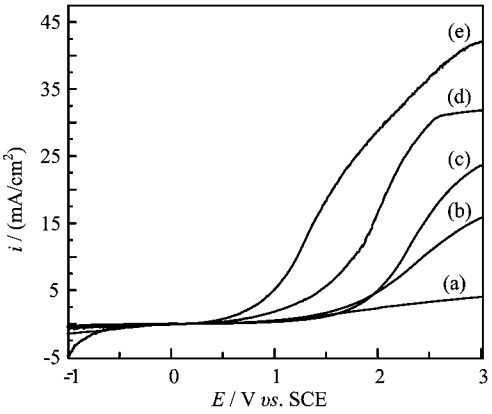

FIG. 3 Potentiodynamic polarization curves of Ta in anhydrous ethanol with different TEA concentration of (a) 0.02 mol/L, (b) 0.04 mol/L, (c) 0.06 mol/L, (d) 0.08 mol/L, and (e) 0.10 mol/L at scan rate of 5 mV/s.

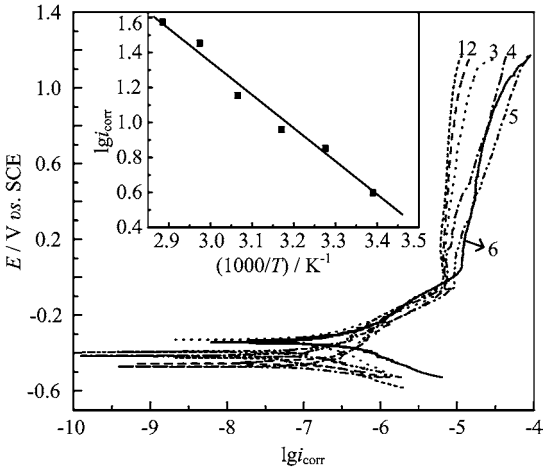

FIG. 4 Tafel curves recorded for tantalum in anhydrous ethanol containing 0.1 mol/L TEA at different temperatures with scan rate of 1 mV/s. The temperatures for curves 1, 2, 3, 4, 5, and 6 are 20, 30, 40, 50, 60, and 70 °C, respectively. Inset is a plot of $\lg i_{\rm corr}$ *vs.* $1/T$.

pit nucleation begins [22].

According to Hoar's theory, the breakdown of the passive film and the initiation of the pitting attack can be ascribed to the adsorption of Cl^- ions on the passive film [23]. The adsorbed aggressive anions, with the assistance of a high electric field, can penetrate the passive layer specifically at its defect points and flaws to reach the base metal surface. Subsequently, the pit growth occurs as a result of the increase in the concentration of Cl^- resulting from its migration [24].

B. Scanning electron microscopy (SEM) characterization

Figure 2 shows the microscopic observations of the electrode surface anodized for various time at 2.5 V. Only several pits appeared in the image after anodization for 2 min. The number of pits sharply increased, and the pits were connected with one another while being anodized for 5 min. The pits became much larger, and large cavities emerged when the electrode was anodized for 60 min. The growth process of the pits is clearly shown on the SEM photographs.

C. Effect of TEA concentration

The influence of TEA concentration on the anodic potentiodynamic polarization curves of tantalum is presented in Fig.3. The increase in the concentration of TEA increases the anodic current density at the same anodic potential. The acceleration effect of TEA may be due to the adsorption of Cl^- on the metal surface and its subsequent participation in active dissolution. Moreover, the breakdown potential $E_{\rm b}$ shifts to negative values with the increase in TEA concentration. These behaviors may be due to the weakening of the passive film as a result of the competition between its formation and the formation of the soluble intermediate, and the increase in the number of aggressive chloride ions that attack the passive layer [25]. Figure 4 presents the Tafel curves at different temperatures. As can be seen, the shape and change trends of each curve looked similar, indicating that dissolution mechanisms did not change at all. With the increase in the solution temperature,

DOI:10.1063/1674-0068/27/04/491-496

the curves shifted to the right, corresponding to a larger current density. The corrosion current density is a parameter that represents the corrosion rate of a material. Thus, the increase in temperature accelerated the corrosion rates of Ta. This promoting effect of the solution temperature on the corrosion process can be explained by the fact that the increase in temperature accelerates the rates of charge transfer, migration, and diffusion of the reactant and product species into and from pits. Moreover, the increase in temperature can enhance the solubility of the passive film.

The apparent activation energy, E_a, of Ta in 0.1 mol/L TEA solution of anhydrous ethanol can be calculated from the following Arrhenius-type equation [26]:

$$\lg i_{corr} = \frac{-E_a}{2.303RT} + A \quad (1)$$

where i_{corr}, the corrosion current density, is calculated through the extrapolation of the linear logarithmic sections of the cathodic and anodic Tafel lines to the point of intersection, R is the universal gas constant, T is the absolute temperature, and A is the pre-exponential factor. A plot of $\lg i_{corr}$ versus $1/T$ is a straight line, as shown in the inset of Fig.4. The E_a obtained from the slope of the straight line is 36 kJ/mol, indicating that the apparent activation energy of the electrochemical reaction near the Tafel region is 36 kJ/mol.

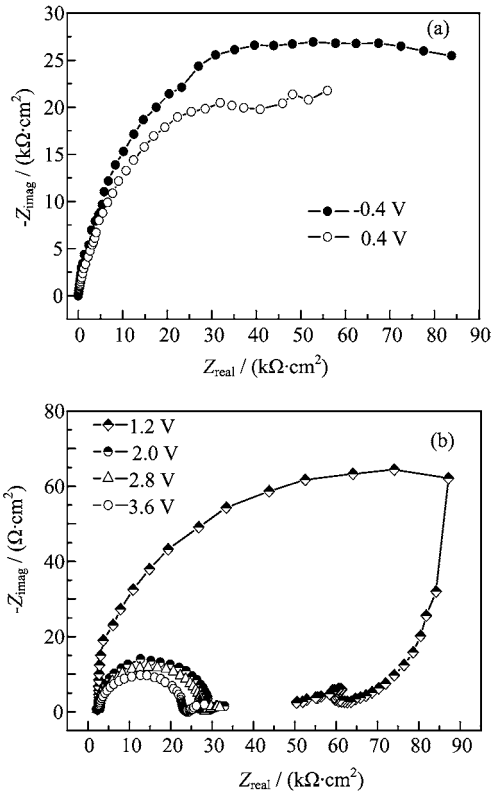

FIG. 5 Nyquist plots of Ta in 0.1 mol/L TEA solution of anhydrous ethanol at various electrode potentials: (a) −0.4 V, 0.4 V, (b) 1.2−3.6 V.

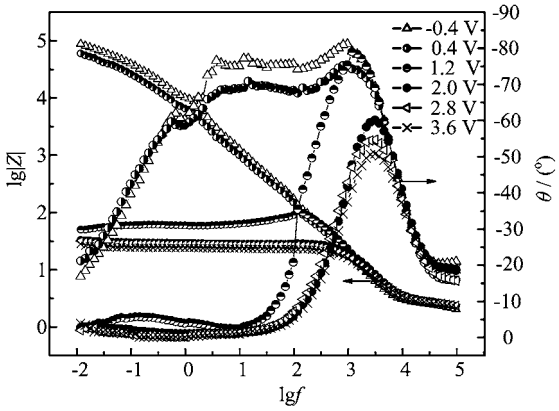

FIG. 6 Bode plots of Ta in 0.1 mol/L TEA solution of anhydrous ethanol at various electrode potentials.

D. Impedance measurements

EIS is a very effective technique that analyzes the various steps involved in an electrochemical reaction by measuring the impedance system response to a small AC potential signal in a wide frequency range [27]. Figures 5 and 6 show the characteristic Nyquist and Bode diagrams of Ta in the 0.1 mol/L TEA solution of anhydrous ethanol at various electrode potentials, respectively. The impedance significantly decreased when the potential increased from −0.4 V to 1.2 V. In fact, the impedance of 1.2 V is three decades smaller than that of −0.4 V, as shown in Fig.6. Moreover, the appearance of an inductive loop at 1.2 V was observed, possibly indicating the commencement of the incubation period of pitting corrosion [28]. However, when the potential was higher than 2.0 V, the tendency to decline clearly slowed down. The inductive loop at the low frequency range was replaced by a nearly ideal Warburg tail, corresponding to the formation of pitting and the appearance of a diffusion-controlled process at high electrode potentials. The slopes of the Bode impedance magnitude plots at intermediate frequencies and the maximum phase angles are close to the ideal values of −1° and 90°, respectively. These divergences from the ideal capacitive behavior may be related to the increase in the rate of passive layer dissolution as a result of its progressive attack, as the potential shifted to be more anodic in the pitting corrosion potential range [25].

The Nyquist and Bode plots show two time constants for all the potentials. They can be modeled using an equivalent circuit (Fig.7), where R_0 is the electrolyte resistance, R_1 is the charge transfer resistance, R_2 is the resistance of the passive layer, L_1 is the inductance, and Q_1 and Q_2 are the constant phase elements related to the capacitance of the double layer and the

DOI:10.1063/1674-0068/27/04/491-496

TABLE I Electrochemical parameters obtained by fitting EIS measurements.

Potential/V	$R_0/(\Omega\cdot cm^2)$	$Q_1/(s^n/\Omega\ cm^2)$	n_1	R_1	$Q_2/(s^n/\Omega\ cm^2)$	n_2	$R_2/(\Omega\cdot cm^2)$	$L_1/(H\cdot cm^2)$
−0.4	2.154	1.277×10^{-5}	0.950	720.778	1.56×10^{-5}	0.499	106743.6	
0.4	2.379	1.124×10^{-5}	0.960	144.713	3.131×10^{-6}	0.650	68893.8	
1.2	2.503	8.050×10^{-6}	0.994	58.227			43.064	0.116
2.0	2.489	6.933×10^{-6}	0.992	26.459	0.567	0.638	5.648	
2.8	2.403	1.326×10^{-5}	0.942	25.472	0.831	0.582	5.345	
3.6	2.234	1.712×10^{-5}	0.916	21.365	1.125	0.618	5.166	

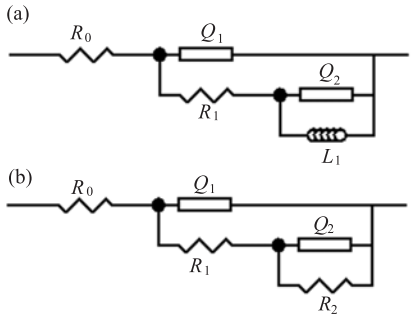

FIG. 7 Equivalent circuits to analyze the experimental data. (a) for 1.2 V, (b) for other potentials.

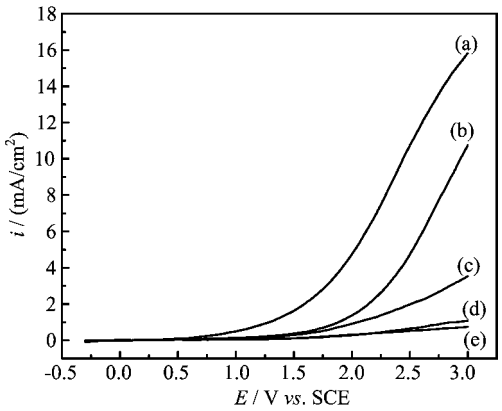

FIG. 8 Effect of water concentration on the polarization curves of Ta in 0.04 mol/L TEA ethanol solution with a scan rate of 5 mV/s. Water concentration with volume percentage is (a) 0, (b) 0.5%, (c) 1%, (d) 2%, and (e) 4%, respectively.

passive film, respectively. The fitting results are listed in Table I. The R_0 values are nearly constant, and the R_1 and R_2 values drastically decreased with the potential as a result of film rapture. This finding further confirms that Ta dissolution is favored, as the anodic potential is made more positive.

E. Effect of water concentration

Water concentration in the ethanol solution, which is very harmful to the electrosynthesis of tantalum alkoxides, greatly reduces yield and current efficiency. Therefore, studying the influence of water content on the corrosion process is necessary. The dependence of the anodic polarization behavior of Ta on water concentration is shown in Fig.8. The curves shifted in the negative direction with increasing water concentration, indicating that passivation was enhanced. The critical pitting potential became more favorable with the increase in water content, consistent with the results of the studies of Ramgopal [29] and Mansfeld [30]. Therefore, in the practical electrosynthesis of tantalum ethoxide, the lowest water content must be maintained to obtain high current efficiency and to avoid the hydrolyzation of the product.

IV. CONCLUSION

Investigations on the corrosion behavior of Ta in TEA ethanol solutions were conducted using potentiodynamic polarization, cyclic voltammetry, and impedance techniques along with SEM. Results show that Ta underwent pitting corrosion in the TEA ethanol solution to a certain extent, depending on the applied anodic potential, anodization time, temperature, and TEA and water concentrations. The current density in the cyclic voltammetry curves very slowly increased with the anodic potential at the early stage of scanning because of spontaneous passivation. The passivity was caused by the presence of a thin oxide film on the anode surface. The electrode retained its passivity up to E_b, when the current increased. The anodic current density increased with the increase in the solution temperature and TEA concentration. The apparent activation energy in the range of the studied temperature was about 36 kJ/mol. SEM images show the growth process of pits on the electrode surface. The impedance spectra exhibited two time constants for all the potentials, and the impedance decreased with increasing potential. The pitting formation process was characterized using EIS. The appearance of an inductive loop corresponded with the incubation period for pitting corrosion, and the presence of another capacitor loop was related to the formation of pits. The critical pitting potential became more positive with increasing water concentration.

DOI:10.1063/1674-0068/27/04/491-496

[1] N. Dharmaraj, H. C. Park, C. H. Kim, P. Viswanathamurthi, and H. Y. Kim, Mater. Res. Bull. **41**, 612 (2006).
[2] S. Ezhilvalavan and T. Y. Tseng, J. Mater. Sci-mater. El. **10**, 9 (1999).
[3] I. V. Sieber and P. Schmuki, J. Electrochem. Soc. **152**, C639 (2005).
[4] C. Wang, L. Fang, G. Zhang, D. M. Zhuang, and M. S. Wu, Thin Solid Films **458**, 246 (2004).
[5] K. Kukli, J. Aarik, A. Aidla, H. Siimon, M. Ritala, and M. Leskel, Appl. Surf. Sci. **112**, 236 (1997).
[6] K. Reuter, F. Zell, and M. Ebner, US Patent 7273943 (2007).
[7] V. A. Shreider, E. P. Turevskaya, N. I. Koslova, and N. Y. Turova, Inorg. Chim. Acta **53**, L73 (1981).
[8] D. Bradley, R. Mehrotra, I. Rothwell, and A. Singh, *Alkoxo and Aryloxo Derivatives of Metals*, London: Academic Press, 18 (2001).
[9] T. Tripp, US Patent 3730857 (1973).
[10] V. A. Shreider, E. P. Turevskaya, N.I. Kozlova, and N. Y. Turova, Russ. Chem. Bull. **30**, 1363 (1981).
[11] N. Y. Turova, A. V. Korolev, D. E. Tchebukov, A. I. Belokon, A. I. Yanovsky, and Y. T. Struchkov, Polyhedron, **15**, 3869 (1996).
[12] S. H. Yang, Y. M. Chen, H. P. Yang, Y. Y. Liu, M. T. Tang, and G. Z. Qiu, Trans. Nonferrous Met. Soc. China **18**, 196 (2008).
[13] S. H. Yang, Z. Q. Pan, Z. H. Li, M. T. Tang, and G. Z. Qiu, Rare Met. Mater. Eng. **35**, 625 (2006).
[14] H. P. Yang, S. H. Yang, Y. N. Cai, G. F. Hou, J. Y. Xia, and M. T. Tang, Trans. Nonferrous Met. Soc. China **21**, 179 (2011).
[15] H. P. Yang, S. H. Yang, Y. N. Cai, G. F. Hou, and M. T. Tang, Electrochim. Acta **55**, 2829 (2010).
[16] M. Berezkin, I. Chernykh, E. Polyakov, and A. Tomilov, Russ. J. Appl. Chem. **79**, 741 (2006).
[17] M. Berezkin, E. Polyakov, V. Turygin, and A. Tomilov, Russ. J. Electrochem. **43**, 1200 (2007).
[18] A. D. Davydov, Electrochim. Acta **46**, 3777 (2001).
[19] S. M. Maeng, *Ph.D. Dissertation*, New Jersey: New Jersey Institute of Technology, (2005).
[20] H. Kaesche, Mater. Corros. **39**, 153 (1988).
[21] M. A. Amin and S. S. A. Rehim, Electrochim. Acta **49**, 2415 (2004).
[22] M. Metikoš-Huković and I. Milošev, J. Appl. Electrochem. **22**, 448 (1992).
[23] T. P. Hoar, D. C. Mears, and G. P. Rothwell, Corros. Sci. **5**, 279 (1965).
[24] H. H. Hassan, S. S. A. Rehim, and N. F. Mohamed, Corros. Sci. **44**, 37 (2002).
[25] H. H. Hassan and K. Fahmy, Int. J. Electrochem. Sci. **3**, 29 (2008).
[26] M. A. M. Ibrahim, S. S. A. Rehim, and M. M. Hamza, Mater. Chem. Phys. **115**, 80 (2009).
[27] T. Du, D. Tamboli, Y. Luo, and V. Desai, Appl. Surf. Sci. **229**, 167 (2004).
[28] C. P. Lee, Y. Y. Chen, C. Y. Hsu, J. W. Yeh, and H. C. Shih, Thin Solid Films **517**, 1301 (2008).
[29] T. Ramgopal, Corrosion **61**, 757 (2005).
[30] F. Mansfeld, J. Electrochem. Soc. **118**, 1412 (1971).

DOI:10.1063/1674-0068/27/04/491-496